The Repression of E2F-1 Is Critical for the Activity of Minerval against Cancer

Jordi Martínez,[1] Antonio Gutiérrez,[1] Jesús Casas, Victoria Lladó, Alicia López-Bellan, Joan Besalduch, Ana Dopazo, and Pablo V. Escribá

Laboratory of Molecular and Cellular Biomedicine, Institut Universitari d'Investigacions en Ciències de la Salut, Associate Unit of the Consejo Superior de Investigaciones Cientificas, Department of Biology, University of the Balearic Islands, Palma de Mallorca, Spain (J.M., J.C., V.L., A.L.-B., P.V.E.); Department of Hematology, Hospital Son Dureta, Palma de Mallorca, Spain (A.G., J.B.); and Centro Nacional de Investigaciones Cardiovasculares, Madrid, Spain (A.D.)

ABSTRACT

The recently discovered anticancer drug Minerval (2-hydroxy-9-cis-octadecenoic acid) is a synthetic fatty acid that modifies the structure of the membrane. This restructuring facilitates the recruitment of protein kinase C (PKC) α to membranes and is associated with the antineoplastic activity of Minerval in cellular and animal models of cancer. Minerval is a derivative of oleic acid (OA) with an enhanced antiproliferative activity in human cancer cells and animal models of cancer, which is associated with PKCα activation and p21^{CIP} overexpression. However, the signaling cascades involved in its pharmacological activity remain largely unknown. Here, we showed that this drug induced cell cycle arrest before entry into S phase, human lung adenocarcinoma (A549) cells accumulating in the G_0/G_1 phase. This cell cycle arrest was associated with a marked decrease in the expression of E2F-1. This transcription factor activates several cell cycle-related genes, and, accordingly, the expression of certain cyclins and cyclin-dependent kinases (cdks) was markedly lower upon exposure to Minerval. The reduced availability of these kinase heterodimers was associated with reduced phosphorylation of the retinoblastoma protein (pRb) observed after drug treatment. Significantly, hypophosphorylated pRb remains bound to E2F-1 and maintains this transcription factor inactive. The modulation of these antiproliferative mechanisms by Minerval explains its anticancer potency, through a new therapeutic strategy that can be used to develop new antitumor drugs. On the other hand, apoptosis did not seem to be involved in its pharmacological mechanism. Interestingly, whereas the changes induced by OA were only modest, they may reflect the beneficial effects of high olive oil intake against cancer.

Minerval (2-hydroxy-9-cis-octadecenoic acid) is a nontoxic synthetic derivative of oleic acid (OA) recently designed by us (Fig. 1a). It impairs proliferation and has antineoplastic effects on cell and animal models of cancer (Martínez et al., 2005). It binds to membrane lipids inducing a structural reorganization of the lipid membrane, which is determined by the "molecular shape" of OA and structural analogs (e.g.,

Minerval) (Funari et al., 2003; Barceló et al., 2004; Martínez et al., 2005). Regulation of the membrane structure by Minerval results in changes in expression, localization, and activity of PKC (Alemany et al., 2004; Martínez et al., 2005). This kinase is a pivotal element in the control of cell growth and development, whose activity has been seen to be involved in the influence of Minerval on cancer cell proliferation. However, the molecular processes that regulate those cell signaling events involved in the pharmacological activity of Minerval remain largely unknown.

Here, we investigated the molecular alterations associated with the antiproliferative activity of Minerval. We found that this synthetic fatty acid impaired cell cycle progress from G_1 to S phase. One of the main transcription factors involved in regulating the genes required for cell cycle progression is E2F-1 (Johnson et al., 1993). A large number of genes involved in the control of the cell cycle and related events

scription factor. These marked and significant decreases of E2F-1 and cyclin/cdk, in addition to hypophosphorylation of pRb, are associated with exit from the cell cycle and account for the antiproliferative effects of Minerval (Fig. 1b). To our knowledge, this is the first report showing that a regulator of the organization of membrane lipids (in fact, a free fatty acid) can control progression of the cell cycle through E2F-1, the overall process being a new mechanism of action.

Materials and Methods

Cell Culture. A549 human lung adenocarcinoma cells were obtained from the American Type Culture Collection (Manassas, VA). A549 cells were maintained at 37°C in a fully humidified atmosphere of 5% CO_2 in air. Monolayer cultures were maintained in exponential growth using 2 mM glutamine-supplemented RPMI 1640 medium, containing 10% bovine calf serum, 100 units/ml penicillin, 100 μg/ml streptomycin, and 0.25 μg/ml amphotericin B. Tissue culture medium and supplements were all purchased from Sigma (Madrid, Spain).

Cell Proliferation Assays. A549 cells were plated at a density of 1.5×10^5 cells in 24-well plates with 0.5 ml of culture medium per well. After incubating overnight to allow cell attachment, the cells were treated with 25 to 100 μM Minerval or 25 to 250 μM OA for 24, 48, and 72 h. At the end of these periods, unattached cells were recovered by centrifugation for 5 min at room temperature and 600g and combined with the adherent cells that had been harvested with 0.05% trypsin in sterile phosphate-buffered saline (PBS, 137 mM NaCl, 2.6 mM KCl, 10 mM Na_2HPO_4, and 1.8 mM KH_2PO_4, at pH 7.3) for 5 min at 37°C and centrifuged as described above. The cells were immediately counted using an automated cell counter (Advia 120; Bayer Diagnostics, Tarrytown, NY), and cell viability was determined by trypan blue exclusion method (0.2% trypan blue in PBS buffer).

Cell Cycle Analysis. Analysis of the cell cycle by flow cytometry was performed on cells treated in the presence or absence (control) of Minerval or OA for 24 h. The cells were then washed twice with PBS, detached by trypsin treatment (see above) and fixed with 100% methanol for 2 h at 4°C. These cells were then centrifuged for 5 min at room temperature and 600g and resuspended in PBS. Finally, cells were incubated for 30 min in the presence of 100 μg/ml ethidium bromide and 100 μg/ml RNase A and analyzed on a Beckman Coulter Epics XL flow cytometer. Cell populations in the different phases of cell cycle (sub-G_1, G_0/G_1, S, and G_2/M) were determined based on their DNA content.

Electrophoresis (SDS-Polyacrylamide Gel Electrophoresis), Immunoblotting, and Protein Quantification. Cells were incubated in the presence or absence of Minerval, as indicated above, in six-well culture plates. The cells were then washed twice with PBS and harvested with a rubber policeman in 300 μl of 10 mM Tris·HCl buffer, pH 7.4, containing 50 mM NaCl, 1 mM $MgCl_2$, 2 mM EDTA, 1% SDS, 5 mM iodoacetamide, and 1 mM phenylmethylsulfonyl fluoride. The cells were homogenized by ultrasound for 10 s at 50 W in a Braun Labsonic U sonicator (20% cycle), and aliquots of 30 μl were removed for total protein quantification. Then, 30 μl of 10× electrophoresis loading buffer (120 mM Tris·HCl buffer, pH 6.8, 4% SDS, 10% β-mercaptoethanol, 50% glycerol, and 0.1% bromphenol blue) was added to the samples, and they were boiled for 3 min. For immunoblotting, 30 μg of total protein from the cell lysates (5–60 μg from control samples for standard curves) was subjected to SDS-polyacrylamide gel electrophoresis and transferred to nitrocellulose membranes (Whatman Schleicher and Schuell, Dassel, Germany). The membranes were incubated with blocking solution for 1 h at room temperature, using PBS buffer containing 5% nonfat dry milk, 0.5% bovine serum albumin, and 0.1% Tween 20 for most immunoblots, or Tris-buffered saline buffer containing 5% nonfat dry milk and 0.1% Tween 20 for phosphorylated pRb detection. The mem-
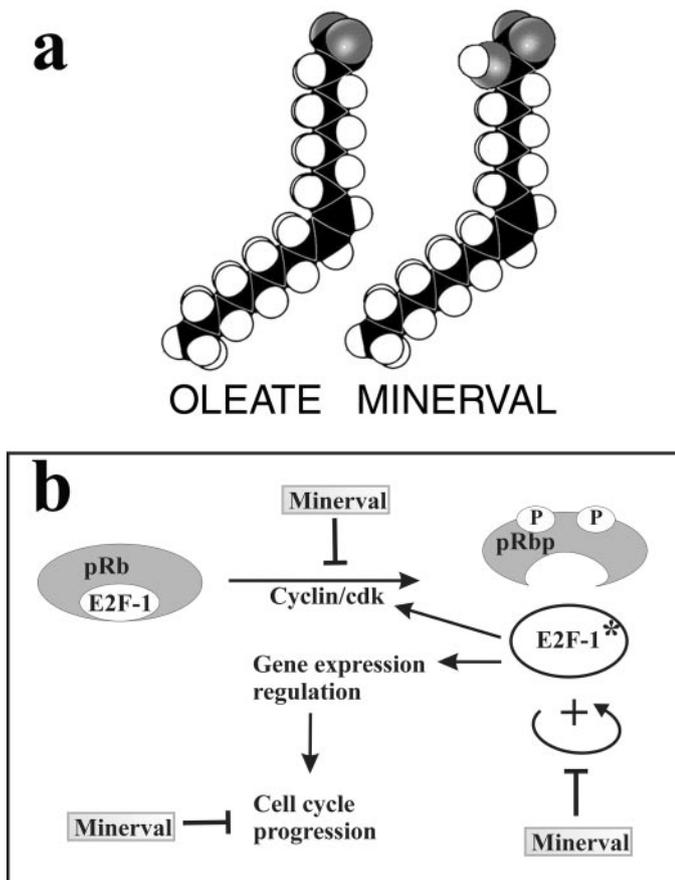

Fig. 1. a, structural comparison of OA and Minerval. In the molecular models, the carbon atoms are shown in black, hydrogen in white, and oxygen in gray. The only difference between both molecules is the oxygen atom on the α carbon of Minerval. b, regulation of the cell cycle progression by E2F-1 and the effects of Minerval. Cell division is associated with an increase in the levels of cyclin/cdk that phosphorylate, among other targets, pRb. Phosphorylated pRb (pRb-p) releases active E2F-1 (E2F-1*), which activates the transcription of several cell cycle-related genes, including E2F-1 itself. The effects induced by Minerval are shown, i.e., hypophosphorylation of pRb, E2F-1 repression by inactivation through pRb binding, and inhibition of the cell cycle progression.

contain regulatory binding sites for E2F-1 (e.g., c-myc, cyclin D3, proliferating cell nuclear antigen, DNA polymerase as well as E2F-1 itself) (Schaley et al., 2000; Li et al., 2003; Ma et al., 2003). Therefore, the dramatic down-regulation of E2F-1 upon exposure to Minerval is likely to be a key molecular event in the mechanism this drug uses to impair cell proliferation (Fig. 1b). The regulatory effects of this transcription factor are modulated by the retinoblastoma protein (pRb), which binds to and inhibits E2F-1. In addition, the pRb/E2F-1 complex induces transcriptional repression of other genes required for cell cycle progression (Young et al., 2003). Indeed, the activity of cyclins and cdks are regulated by this transcription factor. The cyclins and cdks form heterodimers that phosphorylate other cell cycle-related proteins, such as pRb. Phosphorylation of pRb favors the release of active E2F-1, which in turn activates a variety of genes (Dyson, 1998; Young et al., 2003). The reduction in the levels of cyclins and cdks that accumulate after exposure to Minerval are in accordance with the observed hypophosphorylation of pRb, this being a substrate for these kinase complexes. Therefore, in addition to E2F-1 down-regulation, pRb hypophosphorylation contributes to the inhibition of this tran-

branes were then incubated overnight at 4°C in fresh blocking solution containing the specific primary antibodies: monoclonal anti-cyclin D1 (1:500 dilution), monoclonal anti-cyclin D3 (1:1000 dilution), monoclonal anti-cyclin E (1:1000 dilution), monoclonal anti-cdk2 (1:1000 dilution), monoclonal anti-cdk4 (1:1000 dilution), monoclonal anti-pRb (1:500 dilution), and monoclonal anti-E2F-1 (1:1000 dilution) (BD Transduction Laboratories, Heidelberg, Germany), and polyclonal anti-poly ADP-ribose polymerase (anti-PARP, 1:1000 dilution) (Cell Signaling Technology Inc., Beverly, MA). Subsequently, the membranes were incubated with sheep anti-mouse (for monoclonal antibodies) or donkey anti-rabbit (for the polyclonal antiserum) horseradish peroxidase-labeled antiserum (1:2000 dilution in blocking solution) for 1 h at room temperature. The immunoreactive protein bands were detected using the enhanced chemiluminescence Western blotting detection system (GE Healthcare, Piscataway, NJ). Quantification was performed by image analysis, for which four different concentrations of protein from control samples were loaded along with duplicate samples to be tested on 6 × 8-cm 15-well minigels. Four gels were usually processed in parallel. The films were scanned in the transparency mode with a resolution of 42 μm (600 dpi), using the Foto Look 32 software (Agfa Gevaert, Leverkusen, Germany). The integrated optical density of the four control samples of each gel was plotted against the amount of protein loaded. Integrated optical density values were interpolated into the standard curve of their corresponding gels to calculate the percentage of variation with respect to control cells (untreated) as follows:

$$C = 100 \times (P_T/P_R) \tag{1}$$

where C is the cellular concentration of a given protein (100% being the control sample used for the standard curve), P_T is the theoretical amount of protein loaded on the gel (calculated from the standard curves), and P_R is the real amount of protein loaded.

Quantitative Reverse Transcription-Polymerase Chain Reaction (RT-PCR) of mRNA Expression. Quantitative RT-PCR was used to determine the transcriptional modulation of cyclins D1, D3, and E, cdk2 and cdk4, and E2F-1 by Minerval. For this purpose, total RNA was extracted from 3×10^6 A549 cells using the RNeasy Midi kit (QIAGEN, Valencia, CA) according to the manufacturer's instructions. Reverse transcription (RT) reactions were prepared using 1 μg of total RNA, 0.5 μl of oligo(dT) (500 μg/ml), 0.5 μl of

random hexamers (500 μg/ml), and 1 μl of 10 mM dNTPs in a volume of 12 μl. This mixture was heated at 65°C for 5 min and immediately chilled on ice. Then, 4 μl of "5× First-Strand Buffer" (Invitrogen, Carlsbad, CA), 2 μl of 0.1 M dithiothreitol, and 1 μl of "RNase OUT" (recombinant ribonuclease inhibitor; Invitrogen) was added, and the mixture was incubated at 37°C for 2 min. Finally, 1 μl (200 units) of Moloney murine leukemia virus reverse transcriptase (Invitrogen) was added, and the mixture was incubated for 50 min at 37°C. The RT reaction was stopped by heating the tubes at 70°C for 15 min. PCR conditions were first determined in preliminary experiments using a gradient thermal cycler (Eppendorf-5 Prime, Inc., Boulder, CO). The sequence of the primers used, annealing temperatures, the length of the DNA segments, and their corresponding melting temperatures are shown in Table 1. After preliminary calculations of the RNA content by absorbance spectroscopy at 260 nm, a fine calculation of the RNA concentration was performed by quantifying the 18S RNA by PCR using the primers shown in Table 1. Real-time PCR amplifications were carried out in a LightCycler thermal cycler (Roche Diagnostics, Indianapolis, IN) using a LightCycler-FastStart DNA Master SYBR Green I kit (Roche Diagnostics) according to the manufacturer's instructions. An initial denaturation step at 95°C for 5 min preceded thermal cycling. DNA amplification and fluorescence quantification was determined for 30 cycles at 95°C for 3 s, 55–60°C (Table 1) for 7 s and 72°C for 12 s. Fluorescence quantification was carried out at the end of the DNA extension step (72°C) after each temperature cycle because no primer-dimers were produced during the PCRs carried out (as determined by analyses of the melting temperatures for each PCR product after each experiment). Agarose gel electrophoresis was carried out to further characterize PCR products. Data were analyzed using the LightCycler software. For quantification purposes, we used eq. 2 (Pfaffl et al., 2002) as follows:

$$R = \frac{(E_{target})^{\Delta CPtarget(MEANcontrol-MEANminerval)}}{(E_{ref})^{\Delta CPref(MEANcontrol-MEANminerval)}} \tag{2}$$

where R is the ratio between the expression of the gene studied (target) and a housekeeping "reference" gene (ref, 18S RNA), whose expression is not modulated by Minerval (as determined in preliminary experiments). This value (R) was used to calculate the relative expression in Minerval-treated cells with respect to untreated (con-

TABLE 1

RT-PCR primers

The annealing temperature of the RT-PCR is indicated; the rest of PCR conditions are indicated under *Materials and Methods*. The melting temperature and size of each amplicon was determined after each experiment.

	Oligonucleotide	Annealing Temperature	Fragment Size[a]	Fragment Temperature
		°C	bp	°C
E2F-1 (M96577)[b]				
Forward	5′-AGGAGTTCATCAGCCTTTCCC-3′	60		
Reverse	5′-CCCCAAAGTCACAGTCGAAGAG-3′	60	101	88.6
Cyclin D1 (NM05305)				
Forward	5′-TCCTCCTCTTCCTCCTCCTC-3′	55		
Reverse	5′-TCAAGTGTGACCCAGACTGC-3′	55	124	90.7
Cyclin D3 (BC011616)				
Forward	5′-TTTTAGAGGGACCCCAATCC-3′	60		
Reverse	5′-ACCAGCATTCCTTTTGAACG-3′	60	133	84.25
Cyclin E (M73812)				
Forward	5′-TCTGTAAAAGCAAACGCACG-3′	60	124	
Reverse	5′-AGCGGTAAGAAGCAGAGCAG-4′	60		88.3
Cdk2 (NM001798)				
Forward	5′-ATGGACGGAGCTTGTTATCG-3′	60	165	
Reverse	5′-GGAGAGGGTGAGATTAGGGC-3′	60		87.2
Cdk4 (NM000075)				
Forward	5′-CTGGTCGGCTTCAGAGTTTC-3′	60	120	
Reverse	5′-CCCGAAGTTCTTCTGCAGTC-3′	60		83.8
RNA 18S (X01117)				
Forward	5′-GAGGTGAAATTCTTGGACCGG-3′	63		
Reverse	5′-CGAACCTCCGACTTTCGTTCT-3′	63	94	82.7

[a] Size of the PCR product obtained in base pairs.
[b] DNA accession numbers (GenBank) for the corresponding sequence.

trol) cells (percentage of expression $= 100 \times R$; this value was 100 for samples whose expression is identical to that of untreated cells). E_{target} and E_{ref} were the efficiencies of target and reference PCR amplifications, respectively. PCR efficiencies were calculated every experiment for each gene measured by preparing a mixture containing equivalent amounts of the RT reactions from all the samples prepared. This mixture was used as template for PCRs containing 5 pg to 5 ng (four independent reactions) of total RNA. These reactions were submitted to thermal cycling at the same time as reactions from control and Minerval-treated samples. Under our experimental conditions, real-time RT-PCR efficiencies ranked 1.5 to 2, with $E = 2$ being the ideal efficiency (meaning that one PCR "short-product" or amplicon produces two DNA molecules after each cycle). The ΔCP-target(MEAN control $-$ MEAN sample) value corresponded to the difference between the crossing point (CP, PCR cycle where the exponential curve is first detected over the background noise) of the control and the problem PCR curves (mean of three different reactions processed in parallel). Three to six independent experiments were carried out to evaluate the transcriptional regulation of each gene. This method of quantification, based on the determination of the beginning of exponential curves, has proven to be both accurate and reproducible as described previously (Pfaffl et al., 2002). The main trouble for mRNA quantification using real-time RT-PCR techniques is the formation of primer-dimers (Escribá et al., 2004). However, the primer sequences selected for the present study and the experimental conditions used here did not yield undesirable unspecific products. Under these conditions, this method is more convenient and precise than other quantitative approaches based on one-point measurements of PCR amplifications during the exponential phase of the curve or based on endpoint measurements (this latter method being even less accurate than the former).

Statistics. The results are expressed as the mean $\pm$ S.E.M. of at least three independent experiments. The Student's t test or one-way analysis of variance followed by Fisher's tests was used for statistical evaluations. The level of significance was chosen as $P = 0.05$.

Results

Minerval inhibited the proliferation of human lung adenocarcinoma (A549) cells in a time- and dose-dependent manner. After 72 h, 100 μM Minerval inhibited cell proliferation by up to 66 $\pm$ 2% ($P < 0.01$; Fig. 2, a and b). In contrast, 100 μM OA only exerted modest ($<$10%) and nonsignificant ($P > 0.05$) effects on A549 cell proliferation (Fig. 2c). We studied the effect of Minerval on the cell population to determine when the cells entered in cell cycle arrest. Minerval (100 μM, 24 h) induced a significant increase in the number of cells in G_0/G_1 phase, with a concomitant decrease in the cell population in S and G_2 (Fig. 3). These data suggest that Minerval treatment impaired progression through the G_1 checkpoint. In contrast, OA, which is a natural fatty acid and a precursor of Minerval, did not significantly affect cell proliferation (Fig. 3) or the proportion of cells found in different stages of the cell cycle (Fig. 3) at the concentrations of Minerval used. However, at higher concentrations of OA ($\geq$250 μM), inhibition of cell proliferation could be detected (42 $\pm$ 2%, $P < 0.05$,
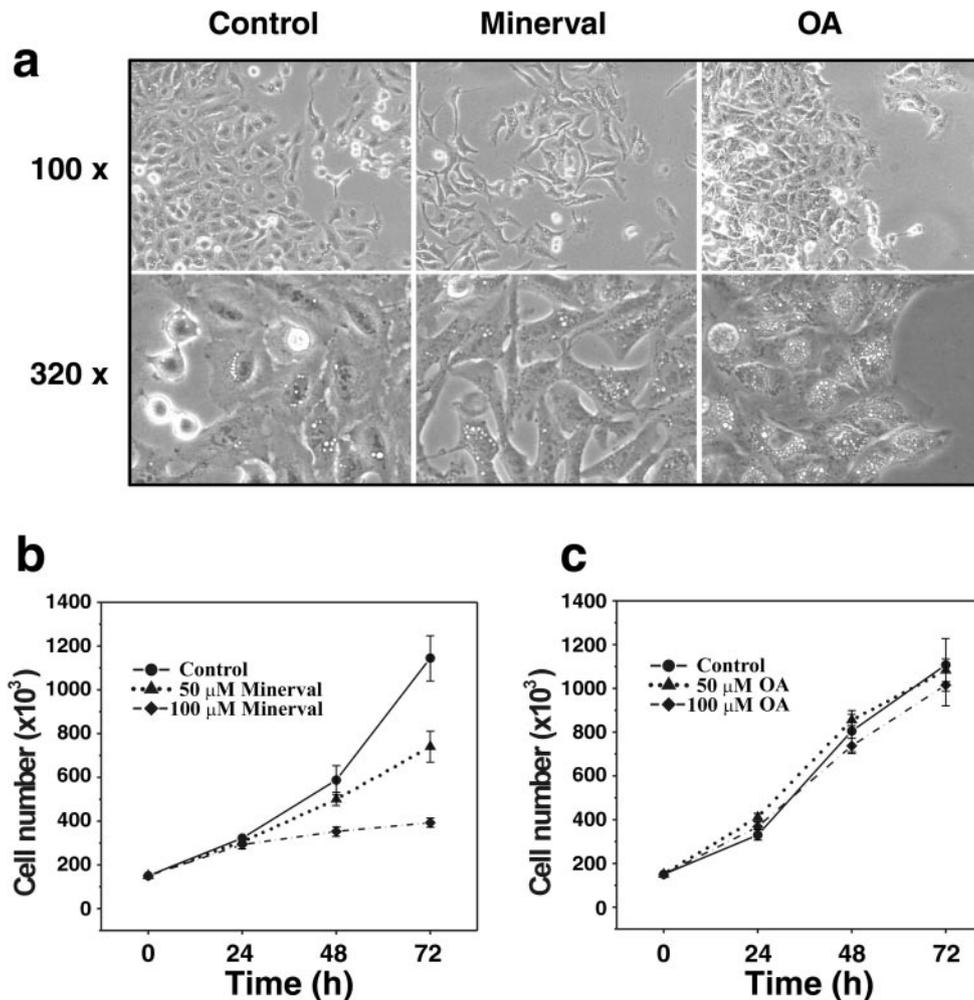

Fig. 2. Effects of Minerval and OA on cell proliferation. a, phase contrast microscopy of A549 cells incubated for 24 h in the presence or absence (control) of 100 μM Minerval or 100 μM OA. The magnification is indicated on the left. Number of A549 cells calculated by flow cytometry in the presence or absence (control) of 50 μM (dotted line) and 100 μM (dashed line) of Minerval (b) or OA (c).
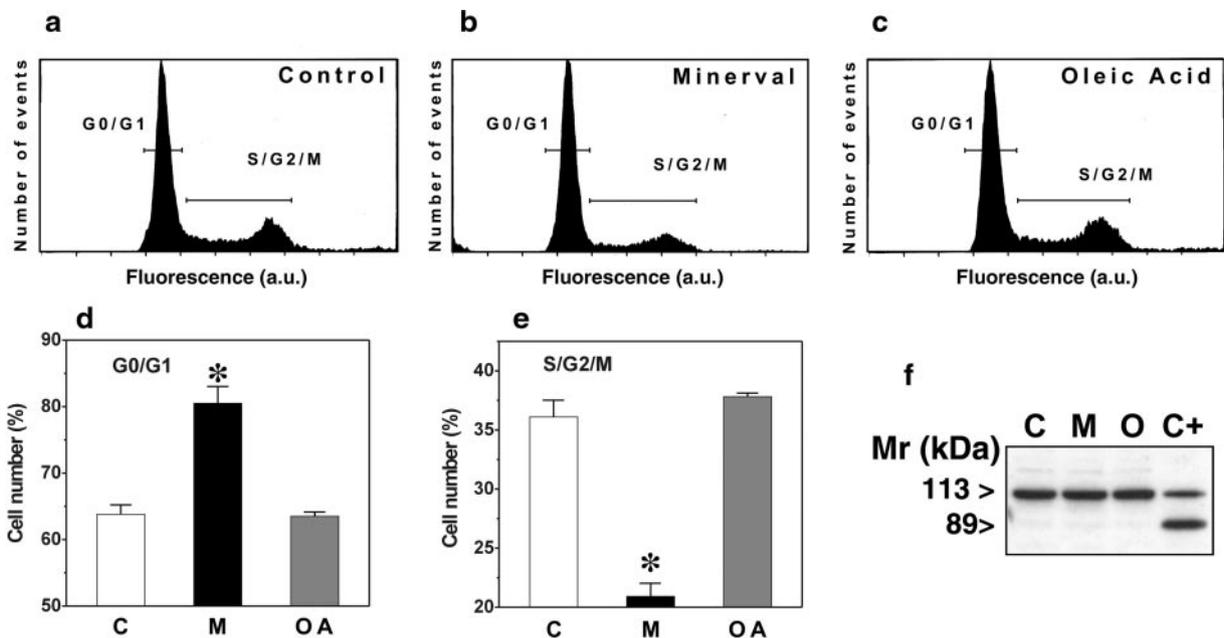
Fig. 3. Effects of Minerval and OA on the cell cycle. DNA content of A549 cells was measured by flow cytometry after a 24-h exposure to Minerval and ethidium bromide staining as indicated under *Materials and Methods*. Histograms of untreated control cells (a) and cells treated with 100 μM of Minerval (b) or OA (c) are shown. The fluorescence values used to calculate the peaks corresponding to the G_0/G_1 and the G_2/M phase are indicated on each histogram. Bar graphs show the percentage of A549 cells in G_0/G_1 (d) and $S/G_2/M$ (e) phase with respect to the total cell number after 24-h in the presence or absence (C) of 100 μM Minerval (M) or OA. The data are the mean $\pm$ S.E.M. values of six independent experiments; *, $P < 0.01$. f, immunoblotting analysis of PARP in A549 cells incubated in the presence or absence of Minerval (M), OA (O), and a positive control of apoptosis (C+).

at 72 h). Flow cytometry highlighted the absence of a significant sub-G_1 population, a peak that is associated with apoptosis (Fig. 3). Furthermore, no PARP fragmentation was observed (Fig. 3). These results indicate that the lower number of cells in the presence of Minerval was due to impaired cell proliferation rather than to apoptosis of A549 cells.

Minerval induced a marked and significant decrease in the expression of the transcription factor E2F-1. After exposure to Minerval, the levels of E2F-1 protein decreased by $90 \pm 4\%$ ($P < 0.001$; Fig. 4a) and the mRNA levels by $55 \pm 5\%$ ($P < 0.01$; Fig. 4b) in A549 cells. In contrast, OA produced only a modest but significant decrease in the accumulation of E2F-1 protein ($20 \pm 1\%$, $P < 0.05$; Fig. 4a). This effect may partially explain the antiproliferative activity of Minerval.

Cell cycle progression is associated with pRb phosphorylation, and hence, the effects of Minerval and OA on the phosphorylation status of pRb were studied by immunoblotting. Exposure to 100 μM Minerval for 24 h induced a marked impairment of pRb phosphorylation and reductions of up to $72 \pm 2\%$ were observed ($P < 0.01$; Fig. 5). The inhibition of pRb phosphorylation by OA (100 μM) after a similar period of time was modest compared with that induced by Minerval ($21 \pm 4\%$, $P < 0.05$; Fig. 5). This inhibition of pRb phosphorylation is in agreement with inhibition of cell cycle progression induced by Minerval. None of these treatments induced significant changes in the accumulation of pRb in the cell (data not shown).

Having determined that the cells accumulated in G_1 phase when exposed to Minerval, we therefore studied its influence on the molecular entities involved in the G_1/S transition. Exposure to 100 μM Minerval for 24 h induced a significant and marked decrease in the accumulation of cyclin D3, cdk2, and cdk4 (reductions of $74 \pm 2\%$, $P < 0.01$; $87 \pm 2\%$, $P <$

0.001; and $46 \pm 20\%$, $P < 0.05$, respectively; Fig. 6a). In contrast, cyclin D1 and cyclin E were not significantly affected by exposure to Minerval. On the other hand, OA did not significantly alter the cellular levels of these proteins under the same experimental conditions (Fig. 6b). A similar effect was observed when the mRNA transcripts encoding these cyclins and cdks were quantified. In this context, RT-PCR analysis showed marked reductions in cyclin D3 and cdk2 transcripts, a modest decrease of cdk4 transcripts, a modest increase of cyclin E mRNA, and a marked increase in cyclin D1 transcripts (Fig. 7).

Discussion

In previous studies, we showed that certain drugs (e.g., daunorubicin and hexamethylene bisacetamide) that are effective against cancer alter the organization of plasma membrane lipids (Escribá et al., 1995, 2002). This modification of the lipid membrane structure has a significant influence on the localization and activity of key signaling proteins, such as PKC. Interestingly, this kinase is known to be involved in the regulation of cell growth of many different cell types. Consequently, we examined how these alterations in membrane structure and PKC activity were affected by a variety of different molecules. In this sense, OA and derivatives (e.g., Minerval) exerted a strong influence on the membrane structure and associated signaling pathways (Funari et al., 2003, Martínez et al., 2005; Yang et al., 2005). However, OA and other fatty acids are good cellular fuels, and they can be degraded through β-oxidation when imported into the mitochondria. This metabolysis impairs the potential pharmacological use of fatty acids, although it does seem that long-term intake of high levels of OA has some protective effect
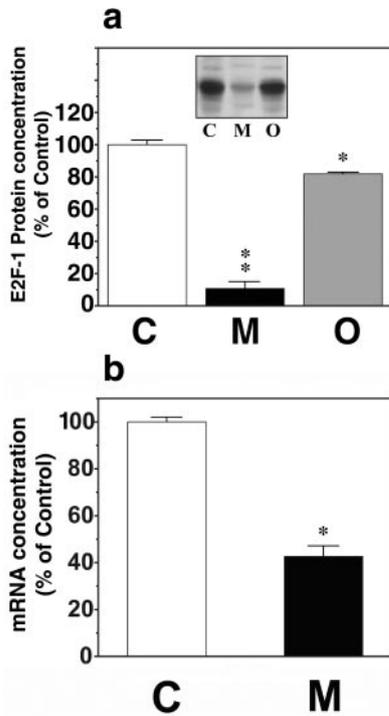
Fig. 4. Effect of Minerval and OA on E2F-1 expression. a, E2F-1 protein levels in cells incubated in the presence of 100 μM Minerval (M) or OA (O) for 24 h. Control cells (C) not exposed to additional fatty acid are also shown. The inset shows representative immunoreactive bands in control (C), Minerval- (M), and OA (O)-treated cells. b, E2F-1 mRNA levels in A549 cells determined by real-time RT-PCR and incubated in the presence or absence (control) of 100 μM Minerval or OA for 24 h. Data shown are the mean $\pm$ S.E.M. values of six independent experiments. $*$, $P <$ 0.01; $**$, $P < 0.001$.
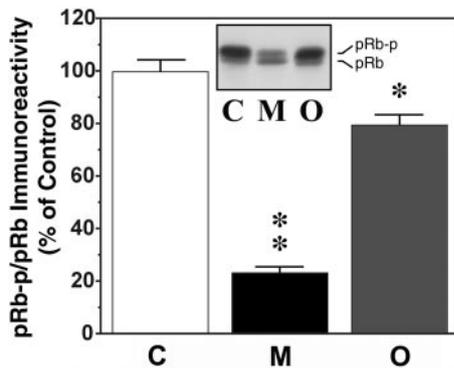

Fig. 5. Effect of Minerval and OA on pRb phosphorylation. A549 cells were incubated in the presence or absence (control, C) of 100 μM Minerval (M) or OA (O) for 24 h. Bars correspond to the ratio between hyperphosphorylated (pRb-p) and hypophosphorylated (pRb) forms of pRb. Data shown are the mean $\pm$ S.E.M. values of four independent experiments. The inset shows a representative immunoblot of pRb and pRb-p from cells incubated in the absence (control, C) or presence of Minerval (M) or OA (O). $*$, $P < 0.05$; $**$, $P < 0.01$.
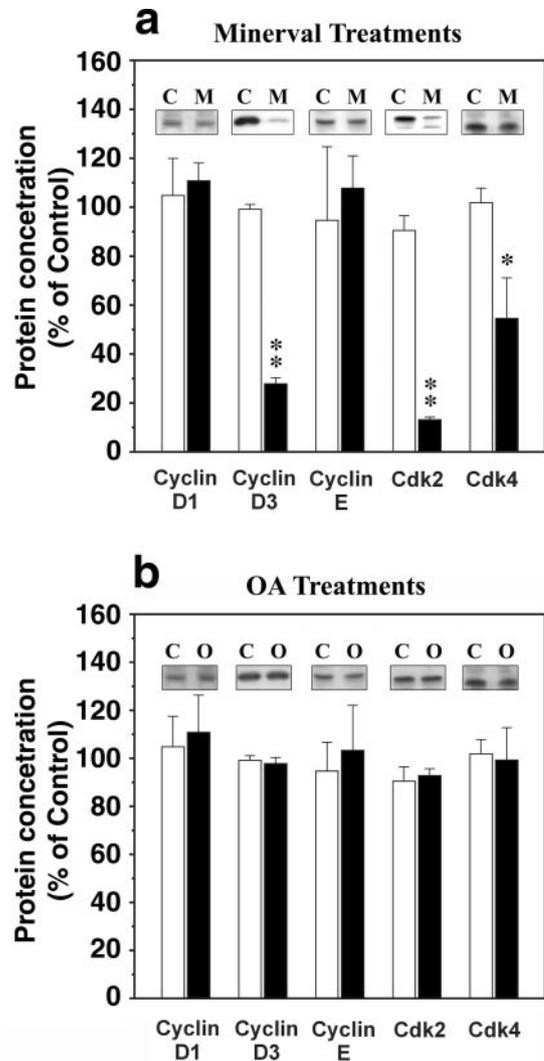

Fig. 6. Effect of Minerval and OA on the expression of cyclin and cdk proteins. Protein concentrations were quantified by immunoblot analysis in cells treated for 24 h with vehicle (open columns), 100 μM Minerval (closed columns, a) or 100 μM OA (closed columns, b). Representative immunoreactive bands are also shown. The data shown are the mean $\pm$ S.E.M. values of five independent experiments. The insets show representative immunoblots of the various cyclins and cdks from control (C), Minerval- (M), and oleic acid (O)-treated A549 cells. For further details, see *Materials and Methods*. $*$, $P < 0.05$; $**$, $P < 0.01$.

although this issue requires further research. Thus, enzymes involved in both processes may not recognize this modified fatty acid, so that its utilization as a source of energy would be decreased, its availability to modify cell signaling increased, and its clearance from cells/organs reduced. Indeed, the presence of this additional oxygen atom markedly increased the antiproliferative activity of Minerval with respect to OA in human adenocarcinoma cells, with no apparent toxic effects (Martínez et al., 2005), which supports the above-mentioned suggestion.

Previous studies have shown that long-term olive oil consumption is associated with a dose-dependent reduction in the incidence of various types of cancer (Martin-Moreno et al., 1994; Llor et al., 2003). The main component of olive oil is OA (about 80%). There is also growing evidence that certain fatty acids exert a protective effect against some types of cancer (Begin and Ells, 1987; Tronstad et al., 2001, 2002; Llor

against the development of tumors (Martin-Moreno et al., 1994). Thus, to overcome this problem, we designed Minerval, a new synthetic OA analog with a hydroxyl group on the α-carbon, a modification that blocks the biological activity of fatty acids (Galbiati et al., 1996). Because this chemical modification is close to the carboxy group of the fatty acid, the mitochondrial import and β-oxidation of Minerval might be impaired (Eaton et al., 1996; Kerner and Hoppel, 2000),
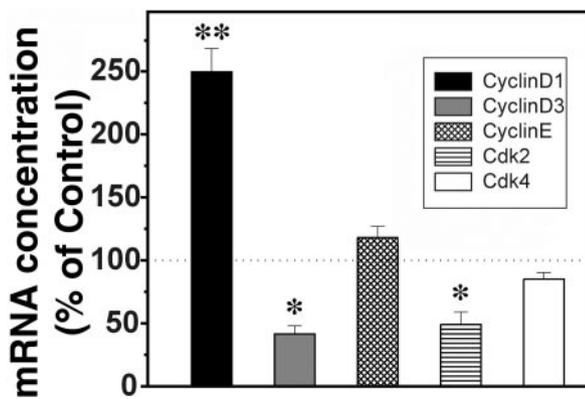
Fig. 7. Effect of Minerval on the relative expression of cyclin and cdk mRNA transcripts. A549 cells were incubated in the presence or absence (control, 100%, dotted line) of 100 μM Minerval for 24 h. Transcriptional rates were quantified by real-time RT-PCR, as described under *Materials and Methods*. The results are the mean $\pm$ S.E.M. values of at least three independent experiments; *, $P < 0.01$.

et al., 2003; Akihisa et al., 2004). In line with these hypotheses, the lipid molecules Edelfosine (Et-18-OCH$_3$) and Miltefosine (hexadecylphosphocholine) are potent antineoplastic drugs targeted to the membrane (Jendrossek and Handrick, 2003). Similarly, polyunsaturated fatty acid (e.g., docosahexaenoic acid and eicosapentaenoic acid) derivatives have anticancer activity (Siddiqui et al., 2005, and references therein). The signal pathways by which these compounds act are not fully understood, so they may share common molecular mechanisms with Minerval.

Recently, we showed that exposure to Minerval inhibits the growth of cancers in both animal models and cultured cells (Martínez et al., 2005). Here, we sought to gain more information about the molecular mechanisms involved in this pharmacological action. We found that Minerval induced cell cycle arrest in G$_0$/G$_1$ and marked and significant decreases of E2F-1, both in terms of protein and mRNA. This transcription factor is involved in the control of a large number of cell cycle-related genes (Young et al., 2003). Thus, an increase in E2F-1 expression is associated with an elevated rate of carcinoma cell growth (Gorgoulis et al., 2002). In turn, its reduction is associated with a lack of proliferation, senescence, and cell differentiation (Saunders et al., 1993; Dimri et al., 1994; Fajas et al., 2002). Therefore, the decrease of E2F-1 levels is probably a key event in the antiproliferative activity of Minerval. To our knowledge, this is the first time that a free fatty acid has been shown to regulate E2F-1 expression. Likewise, the modest decrease of E2F-1 levels and pRb phosphorylation induced by OA might be involved in the protective effects of olive oil against cancer (Martin-Moreno et al., 1994).

Control of the cell cycle involves a number of revision checkpoints. Analysis of the DNA content in A549 cells by flow cytometry showed an accumulation of cells in the G$_0$/G$_1$ phase after exposure to Minerval. This result suggests that Minerval-treated cells exit from the cell cycle before they enter S phase, possibly due to their incapacity to overcome the G$_1$ checkpoint. Cyclins D and E as well as cdk2 and cdk4 are involved in the progression from G$_1$ to S phase (Sherr, 1996). These cyclins and cdks form heterodimers that regulate cell cycle progression through phosphorylation of target proteins. Interestingly, the genes encoding cdk and cyclins

are regulated by E2F-1 and other members of the E2F family (Gorgoulis et al., 2002; Ma et al., 2003). Therefore, we studied what effect Minerval had on their cellular concentrations. We found that Minerval induced marked reductions of cyclin D3, cdk2, and cdk4, which might affect the G$_1$/S phase transition. In most systems, the regulation of cell cycle progression is mainly due to changes in the levels of cyclins, whereas the cellular concentrations of cdks are maintained constant. However, in certain cancer cells, cell cycle arrest is associated with reductions of both cyclins and cdks (Strobeck et al., 2000). Minerval clearly modulated the expression of cdk2 and cdk4 (protein and mRNA levels). The reduction in the levels of these kinases probably amplified the antiproliferative effects of down-regulating cyclin D3. In agreement with the present results, inhibition of these kinases impairs cell proliferation (Keshamouni et al., 2004). In contrast, the levels of cyclin D1 mRNA were higher in the presence of the drug. However, the cellular protein concentration of cyclin D1 was not significantly altered by Minerval treatments. This result supports the involvement of proteasome-mediated degradation, possibly also involved in the above-mentioned down-regulation of cyclins and cdks as suggested previously (Martínez et al., 2005). Finally, cyclin E remained unaffected by exposure to Minerval, indicating that this protein was not involved in its activity.

Hypophosphorylated pRb acts as a switch for cell cycle progression, holding cells in G$_1$ until they are ready to progress into S phase. It binds to several key regulators of cell cycle progression, including members of the E2F family of transcription factors (Mundle and Saberwal, 2003). When pRb is bound to E2F-1, it not only inhibits E2F-1-mediated transcriptional activation but also represses the transcription of a large number of cell cycle-related genes (Mundle and Saberwal, 2003; Young et al., 2003). Under the appropriate conditions, pRb phosphorylation at the G$_1$/S phase transition induces the release of active E2F-1 (Slansky et al., 1993; Ohtani et al., 1995; Ishida et al., 2001; Muller et al., 2001). Because cyclin/cdk heterodimers regulate pRb phosphorylation (Lundberg and Weinberg, 1998), the hypophosphorylated state of pRb induced by Minerval could be due to their down-regulation.

The changes here reported in E2F-1, cyclins, cdks, and pRb are consistent with the reduced proliferation in the presence of Minerval. In this context, Minerval would impair cell proliferation through at least two feedback mechanisms. On one hand, E2F-1 regulates its own expression, such that the low levels of E2F-1 protein are associated with low transcriptional rates of E2F-1 and cell cycle-related genes (Fig. 1b). In contrast, E2F-1 reduction results in down-regulation of cyclins and cdks (Fig. 1b). This event would produce a decrease in pRb phosphorylation, which would promote the accumulation of high levels of the cell cycle inhibitory complex E2F-1/pRb. The binding of pRb to E2F-1 further reduces its capacity to activate the transcription of cell cycle-related genes (Dyson, 1998) and represses the expression of certain genes required for cell cycle progression (Young et al., 2003). By contrast to cell proliferation, Minerval did not induce apoptosis in A549 cells as deduced by the lack of caspase activation, DNA laddering (data not shown), poly(ADP-ribose) polymerase degradation, sub-G$_0$ cell cytometry peaks, or apoptotic bodies.

Alterations in membrane structure regulate the localiza-

tion and activity of peripheral proteins involved in cell proliferation (Escribá et al., 1995, 1997; Vögler et al., 2004; Martínez et al., 2005; Yang et al., 2005). An increase of the membrane nonlamellar phase propensity favors recruitment and subsequent activation of PKC. Minerval binds to membranes and increases their nonlamellar phase propensity, inducing recruitment and moderate activation of PKC in model (liposome) and A549 cell membranes (Barceló et al., 2004; Martínez et al., 2005). PKC activates the cell cycle inhibitor p21^{CIP} (Kashiwagi et al., 2000) and also inhibits E2F during G_1 phase (Nakaigawa et al., 1996), being therefore upstream E2F-1. This effect of Minerval on the membrane lipid organization is of structural nature. Indeed, the structural analog of Minerval, OA, induces similar modifications on the membrane structure, whereas the structurally unrelated analogs, elaidic and stearic acids, do not significantly influence the membrane lipid organization (Funari et al., 2003; Prades et al., 2003; Barceló et al., 2004). Moreover, OA but not elaidic and stearic acids modulate cell signaling upon membrane structure regulation (Yang et al., 2005). The lesser anticancer activity of OA might be due to its use as energy source, as discussed above. The antiproliferative activity of Minerval is associated with a moderate activation of PKC. A huge PKC activation, such as the one provided by phorbol esters, has opposite effects on cell proliferation. Indeed, in certain types of tumors there have been described overexpressions of PKC isozymes (Kamimura et al., 2004). Therefore, in these tumors Minerval would possibly lack of antiproliferative activity. However, other noncytotoxic mechanisms could be involved in its anticancer action, which may justify the broad range of tumors that respond to treatments with this drug. The present data also explain in part how the modulation of membrane structure by Minerval or other anticancer lipid drugs may affect the regulation of gene expression (Escribá et al., 1995, 2002; Jendrossek and Handrick, 2003; Siddiqui et al., 2005). Other possible mechanisms for the pharmacological activity of Minerval, such as the modification of fatty acid metabolism, the stimulation of peroxidative cell damage, or the modification of the lipid composition of the membrane, should not be discarded (Gonzalez et al., 1993; Belury, 2002; Prades et al., 2003). However, under the experimental conditions used, apoptosis did not seem to be involved in the antineoplastic activity of Minerval in A549 cells.

In summary, the impairment of the cell cycle progression induced by Minerval is associated with the down-regulation of E2F-1, cyclins, and cdks and a reduction in the phosphorylation of pRb. The present results are relevant because they 1) characterize relevant molecular mechanisms involved in the anticancer activity of Minerval, and they 2) show molecular events regulated upon membrane structure modulation. In this context, Minerval does not belong to any of the known groups of anticancer drugs and establishes a novel therapeutic approach that can be applied to develop anticancer drugs with low toxicity.

References

Akihisa T, Tokuda H, Ogata M, Ukiya M, Iizuka M, Suzuki T, Metori K, Shimizu N, and Nishino H (2004) Cancer chemopreventive effects of polyunsaturated fatty acids. *Cancer Lett* **205:**9–13.

Alemany R, Terés S, Baamonde C, Benet M, Vögler O, and Escribá PV (2004) 2-Hydroxyoleic acid: a new hypotensive molecule. *Hypertension* **43:**249–254.

Barceló F, Prades J, Funari SS, Frau J, Alemany R, and Escribá PV (2004) The hypotensive drug 2-hydroxyoleic acid modifies the structural properties of model membranes. *Mol Membr Biol* **21:**261–268.

Begin ME and Ells G (1987) Effects of C18 fatty acids on breast carcinoma cells in culture. *Anticancer Res* **7:**215–217.

Belury MA (2002) Inhibition of carcinogenesis by conjugated linoleic acid: potential mechanisms of action. *Nutrition* **132:**2995–2998.

Dimri GP, Hara E, and Campisi J (1994) Regulation of two E2F-related genes in presenescent and senescent human fibroblasts. *J Biol Chem* **269:**16180–16186.

Dyson N (1998) The regulation of E2F by pRB-family proteins. *Genes Dev* **12:**2245–2262.

Eaton S, Bartlett K, and Pourfarzam M (1996) Mammalian mitochondrial β-oxidation. *Biochem J* **320:**345–357.

Escribá PV, Morales P, and Smith A (2002) Membrane phospholipids reorganization differentially regulates metallothionein and heme oxygenase by heme-hemopexin. *DNA Cell Biol* **21:**355–364.

Escribá PV, Ozaita A, and García-Sevilla JA (2004) Increased mRNA expression of α_{2A}-adrenoceptors, serotonin receptors and μ-opioid receptors in the brains of suicide victims. *Neuropsychopharmacology* **29:**1512–1521.

Escribá PV, Ozaita A, Ribas C, Miralles A, Fodor E, Farkas T, and García-Sevilla JA (1997) Role of lipid polymorphism in G protein-membrane interactions: nonlamellar-prone phospholipids and peripheral protein binding to membranes. *Proc Natl Acad Sci USA* **94:**11375–11380.

Escribá PV, Sastre M, and García-Sevilla JA (1995) Disruption of cellular signaling pathways by daunomycin through destabilization of nonlamellar membrane structures. *Proc Natl Acad Sci USA* **92:**7595–7599.

Fajas L, Landsberg RL, Huss-Garcia Y, Sardet C, Lees JA, and Auwerx J (2002) E2Fs regulate adipocyte differentiation. *Dev Cell* **3:**39–49.

Funari SS, Barceló F, and Escribá PV (2003) Effects of oleic acid and its congeners, elaidic and stearic acids, on the structural properties of phosphatidylethanolamine membranes. *J Lipid Res* **44:**567–575.

Galbiati F, Guzzi F, Magee AI, Milligan G, and Parenti M (1996) Chemical inhibition of myristoylation of the G-protein Gi$_1$ alpha by 2-hydroxymyristate does not interfere with its palmitoylation or membrane association. Evidence that palmitoylation, but not myristoylation, regulates membrane attachment. *Biochem J* **313:**717–720.

Gonzalez MJ, Schemmel RA, Dugan L Jr, Gray JI, and Welsch CW (1993) Dietary fish oil inhibits human breast carcinoma growth: a function of increased lipid peroxidation. *Lipids* **28:**827–832.

Gorgoulis, VG, Zacharatos P, Mariatos G, Kotsinas A, Bouda M, Kletsas D, Asimacopoulos PJ, Agnantis N, Kittas C, and Papavassiliou AG (2002) Transcription factor E2F-1 acts as a growth-promoting factor and is associated with adverse prognosis in non-small cell lung carcinomas. *J Pathol* **198:**142–156.

Ishida S, Huang E, Zuzan H, Spang R, Leone G, West M, and Nevins JR (2001) Role for E2F in control of both DNA replication and mitotic functions as revealed from DNA microarray analysis. *Mol Cell Biol* **21:**4684–4699.

Jendrossek V and Handrick R (2003) Membrane targeted anticancer drugs: potent inducers of apoptosis and putative radiosensitisers. *Curr Med Chem Anticancer Agents* **3:**343–353.

Johnson DG, Schwarz JK, Cress WD, and Nevins JR (1993) Expression of transcription factor E2F1 induces quiescent cells to enter S phase. *Nature (Lond)* **365:**349–352.

Kamimura K, Hojo H, and Abe M (2004) Characterization of expression of protein kinase C isozymes in human B-cell lymphoma: relationship between its expression and prognosis. *Pathol Int* **54:**224–230.

Kashiwagi M, Ohba M, Watanabe H, Ishino K, Kasahara K, Sanai Y, Taya Y, and Kuroki T (2000) PKCε associates with cyclin E/cdk2/p21 complex, phosphorylates p21 and inhibits cdk2 kinase in keratinocytes. *Oncogene* **19:**6334–6341.

Kerner J and Hoppel C (2000) Fatty acid import into mitochondria. *Biochim Biophys Acta* **1486:**1–17.

Keshamouni VG, Reddy RC, Arenberg DA, Joel B, Thannickal VJ, Kalemkerian GP, and Standiford TJ (2004) Peroxisome proliferator-activated receptor-gamma activation inhibits tumor progression in non-small-cell lung cancer. *Oncogene* **23:**100–108.

Li YY, Wang L, and Lu CD (2003) An E2F site in the 5′-promoter region contributes to serum-dependent up-regulation of the human proliferating cell nuclear antigen gene. *FEBS Lett* **544:**112–118.

Llor X, Pons E, Roca A, Alvarez M, Mane J, Fernandez-Banares F, and Gassull MA (2003) The effects of fish oil, olive oil, oleic acid and linoleic acid on colorectal neoplastic processes. *Clin Nutr* **22:**71–79.

Lundberg AS and Weinberg RA (1998) Functional inactivation of the retinoblastoma protein requires sequential modification by at least two distinct cyclin-cdk complexes. *Mol Cell Biol* **18:**753–761.

Ma Y, Yuan J, Huang M, Jove R, and Cress WD (2003) Regulation of the cyclin D3 promoter by E2F1. *J Biol Chem* **278:**16770–16776.

Martínez J, Vögler O, Casas J, Barceló F, Alemany R, Prades J, Nagy T, Baamonde C, Kasprzyk G, Terés S, et al. (2005) Membrane structure modulation, protein kinase Cα activation and anticancer activity of Minerval. *Mol Pharmacol* **67:**531–540.

Martin-Moreno JM, Willett WC, Gorgojo L, Banegas JR, Rodriguez-Artalejo F, Fernandez-Rodriguez JC, Maisonneuve P, and Boyle P (1994) Dietary fat, olive oil intake and breast cancer risk. *Int J Cancer* **58:**774–780.

Muller H, Bracken AP, Vernell R, Moroni MC, Christians F, Grassilli E, Prosperini E, Vigo E, Oliner JD, and Helin K (2001) E2Fs regulate the expression of genes involved in differentiation, development, proliferation and apoptosis. *Genes Dev* **15:**267–285.

Mundle SD and Saberwal G (2003) Evolving intricacies and implications of E2F1 regulation. *FASEB J* **17:**569–574.

Nakaigawa N, Hirai S, Mizuno K, Shuin T, Hosaka M, and Ohno S (1996) Differential effects of overexpression of PKCα and PKCδ/ε on cellular E2F activity in late G_1 phase. *Biochem Biophys Res Commun* **222:**95–100.

Ohtani K, DeGregori J, and Nevins JR (1995) Regulation of the cyclin E gene by transcription factor E2F1. *Proc Natl Acad Sci USA* **92:**12146–12150.

Pfaffl MW, Horgan GW, and Dempfle L (2002) Relative expression software tool (REST) for group-wise comparison and statistical analysis of relative expression results in real-time PCR. *Nucleic Acids Res* **30:**e36.

Prades J, Funari SS, Escribá PV, and Barceló F (2003) Effects of unsaturated fatty acids and triacylglycerols on phosphatidylethanolamine membrane structure. *J Lipid Res* **44:**1720–1727.

Saunders NA, Smith RJ, and Jetten AM (1993) Regulation of proliferation-specific and differentiation-specific genes during senescence of human epidermal keratinocyte and mammary epithelial cells. *Biochem Biophys Res Commun* **197:**46–54.

Schaley J, O'Connor RJ, Taylor LJ, Bar-Sagi D, and Hearing P (2000) Induction of the cellular E2F-1 promoter by the adenovirus E4–6/7 protein. *J Virol* **74:**2084–2093.

Sherr CJ (1996) Cancer cell cycles. *Science (Wash DC)* **274:**1672–1677.

Siddiqui RA, Zerouga M, Wu M, Castillo A, Harvey K, Zaloga GP, and Stillwell W (2005) Anticancer properties of propofol-dosahexaenoate and propofol-eicosapentaenoate on breast cancer cells. *Breast Cancer Res* **7:**R645–R654.

Slansky JE, Li Y, Kaelin WG, and Farnham PJ (1993) A protein synthesis-dependent increase in E2F1 mRNA correlates with growth regulation of the dihydrofolate reductase promoter. *Mol Cell Biol* **13:**1610–1618.

Strobeck MW, Fribourg AF, Puga A, and Knudsen ES (2000) Restoration of retino-blastoma mediated signaling to Cdk2 results in cell cycle arrest. *Oncogene* **19:**1857–1867.

Tronstad KJ, Berge K, Dyroy E, Madsen L, and Berge RK (2001) Growth reduction in glioma cells after treatment with tetradecylthioacetic acid: changes in fatty acid metabolism and oxidative status. *Biochem Pharmacol* **61:**639–649.

Tronstad KJ, Bruserud O, Berge K, and Berge RK (2002) Antiproliferative effects of a non-β-oxidizable fatty acid, tetradecylthioacetic acid, in native human acute myelogenous leukemia blast cultures. *Leukemia* **16:**2292–2301.

Vögler O, Casas J, Capó D, Nagy T, Borchert G, Martorell G, and Escribá PV (2004) The Gβγ dimer drives the interaction of heterotrimeric Gi proteins with nonlamellar membrane structures. *J Biol Chem* **279:**36540–36545.

Yang Q, Alemany R, Casas J, Kitajka K, Lanier SM, and Escribá PV (2005) Influence of the membrane lipid structure on signal processing via G protein-coupled receptors. *Mol Pharmacol* **68:**210–217.

Young AP, Nagarajan R, and Longmore GD (2003) Mechanisms of transcriptional regulation by Rb-E2F segregate by biological pathway. *Oncogene* **22:**7209–7217.

Address correspondence to: Dr. Pablo V. Escribá, Laboratory of Molecular and Cellular Biomedicine, Associate Unit of the "Instituto de la Grasa" (CSIC), IUNICS, Department of Biology, University of the Balearic Islands, Ctra. de Valldemossa Km 7.5, E-07122 Palma de Mallorca, Spain. E-mail: pablo.escriba@uib.es